ACCOUNTS of chemical research

Article

pubs.acs.org/accounts

A Theoretical and Experimental Approach for Correlating Nanoparticle Structure and Electrocatalytic Activity

Rachel M. Anderson,[†,‡] David F. Yancey,[†,‡] Liang Zhang,[†,§] Samuel T. Chill,[†,§] Graeme Henkelman,*[,†,§] and Richard M. Crooks*[,†,‡]

[†]Department of Chemistry, [‡]Texas Materials Institute, and [§]Institute for Computational and Engineering Sciences, The University of Texas at Austin, 105 E. 24th St., Stop A5300, Austin, Texas 78712-1224, United States

CONSPECTUS: The objective of the research described in this Account is the development of high-throughput computational-based screening methods for discovery of catalyst candidates and subsequent experimental validation using appropriate catalytic nanoparticles. Dendrimer-encapsulated nanoparticles (DENs), which are well-defined 1−2 nm diameter metal nanoparticles, fulfill the role of model electrocatalysts.

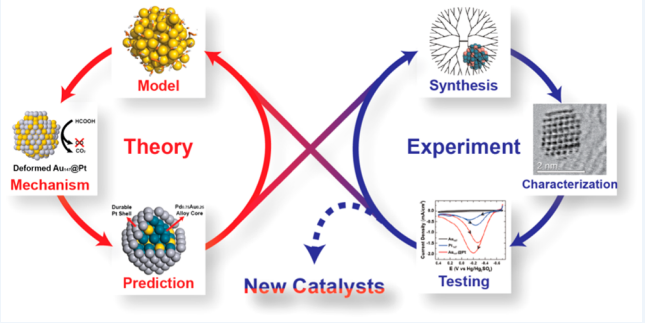

Effective comparison of theory and experiment requires that the theoretical and experimental models map onto one another perfectly. We use novel synthetic methods, advanced characterization techniques, and density functional theory (DFT) calculations to approach this ideal. For example, well-defined core@shell DENs can be synthesized by electrochemical underpotential deposition (UPD), and the observed deposition potentials can be compared to those calculated by DFT. Theory is also used to learn more about structure than can be determined by analytical characterization alone. For example, density functional theory molecular dynamics (DFT-MD) was used to show that the core@shell configuration of Au@Pt DENs undergoes a surface reconstruction that dramatically affects its electrocatalytic properties. A separate Pd@Pt DENs study also revealed reorganization, in this case a core−shell inversion to a Pt@Pd structure. Understanding these types of structural changes is critical to building correlations between structure and catalytic function.

Indeed, the second principal focus of the work described here is correlating structure and catalytic function through the combined use of theory and experiment. For example, the Au@Pt DENs system described earlier is used for the oxygen reduction reaction (ORR) as well as for the electro-oxidation of formic acid. The surface reorganization predicted by theory enhances our understanding of the catalytic measurements. In the case of formic acid oxidation, the deformed nanoparticle structure leads to reduced CO binding energy and therefore improved oxidation activity. The final catalytic study we present is an instance of theory correctly predicting (in advance of the experiments) the structure of an effective DEN electrocatalyst. Specifically, DFT was used to determine the optimal composition of the alloy-core in AuPd@Pt DENs for the ORR. This prediction was subsequently confirmed experimentally. This study highlights the major theme of our research: the progression of using theory to rationalize experimental results to the more advanced goal of using theory to predict catalyst function a priori. We still have a long way to go before theory will be the principal means of catalyst discovery, but this Account begins to shed some light on the path that may lead in that direction.

INTRODUCTION

An emerging strategy for discovering the next generation of catalysts involves utilizing high-level computational methods to predict and screen structure/function relationships. This is due in large part to rapidly advancing computational speed and accessibility. However, a key element in the computational paradigm is the need for well-defined experimental models against which theoretical approaches can be validated. Here, we discuss innovative methods we, and others, have been using to connect theoretical and experimental methods into an integrated research program. If this connection can be made sufficiently efficient and robust, then we envision that catalyst discovery and optimization will be accelerated.

Experimental control of catalyst structure is a prerequisite for effective comparison of theory and experiment. The simplest model system is a perfect, infinite single crystal, and materials approaching this ideal have been profitably studied for many years.[1−6] Usually, however, nanoparticle models are more closely related to real catalytic systems, and hence, there has been much emphasis in recent years on developing a better understanding of their properties. One approach to this problem has been to focus on nanoparticles having facets that are sufficiently large that their catalytic properties approximate bulk, single-crystal surfaces.[7] Indeed, this is the basis for the extensive interest in shape-controlled

Received: March 12, 2015
Published: May 4, 2015

DOI: 10.1021/acs.accounts.5b00125
Acc. Chem. Res. 2015, 48, 1351−1357

nanoparticles, where the facets generally dominate catalytic behavior.[8]

As the size of a nanoparticle decreases, however, edge and corner atoms begin to contribute to its catalytic properties and deviations from bulk behavior are observed. This type of behavior is apparent for metal particles having sizes of <3 nm, but the most interesting size range is from ∼1−2 nm. There are two reasons for this. First, very slight changes to the structure or composition of particles in this size range, or the addition or deletion of a few atoms, can have a dramatic effect on catalysis. Second, particles that contain 30−300 atoms are large enough to effectively characterize but small enough to be analyzed in their entirety using first-principles theory. Of course, there are also problems. For example, such small particles are often unstable and even if they are stable, their native structure may be altered during catalytic reactions. This means that experimental characterization is difficult and best carried out in situ. Additionally, direct comparison of theory and experiment implies that all nanoparticles in an ensemble are uniform, and this ideal situation can only be approximated, to a greater or lesser extent, at the present time.

One established approach for predicting catalyst activity is through the use of a single thermodynamic descriptor, which acts as a proxy for reaction rate. For example, in the case of the oxygen reduction reaction (ORR), a complex multistep reaction can be represented by the binding energy of atomic oxygen on a metal surface.[9] Within this formalism, there is an ideal binding energy that balances the energy of dissociative adsorption of molecular oxygen and desorption of products. The best candidates are found to have an intermediate oxygen binding energy, resulting in a "volcano"-shaped plot of activity versus binding energy.[10] This same general strategy has been employed for reactions such as water oxidation[11,12] (OH binding energy), methanol oxidation[13] (CO and OH binding energies), and hydrogen evolution[14] (H binding energy). On a bulk surface, this treatment is relatively simple because of the uniformity of the surface structure, but the same approach can be applied to nanoparticles on which a greater variety of binding sites are present. Of the many unique sites on nanoparticles, the most catalytically active can be determined by calculating and comparing the binding energies of the model reaction intermediate or product on each distinctive surface location.

As alluded to earlier, a principal difficulty inherent to correlating experimental catalytic measurements to theory is the polydisperse nature of nanoparticles. There are only three possible solutions to this problem: (1) develop synthetic methods that result in uniform distributions of particle size, composition, and structure; (2) develop theory and calculations that are able to take into account polydispersity; (3) develop methods for carrying out catalytic measurements on just one, or perhaps a few, well-defined nanoparticles. There are significant problems associated with all of these approaches, but some progress has been made. For example, mass-selected particle syntheses result in very good mass uniformity.[15] Likewise, a few studies have been reported involving catalytic measurements on single particles, but the particles are typically rather large and it has not been possible to correlate catalytic rates with nanoparticle structure.[16,17] In addition to the problem of polydispersity, there is another difficulty associated with understanding the catalytic properties of 1−2 nm particles: some kind of capping ligand is required to control growth and minimize agglomeration. Such ligands affect nanoparticle electronic properties, reactant access to surface atoms, and in many cases composition and structure as well.

To begin to address some of the aforementioned problems, we developed a class of materials known as dendrimer-encapsulated nanoparticles (DENs).[18−22] DENs are nearly monodisperse nanoparticles with tunable sizes (from just a few atoms[23,24] to ∼300 atoms) and compositions.[20−22] DENs in the size range of ∼0.8 to ∼2.2 nm are large enough to be characterized experimentally and tested for their catalytic properties, but also small enough to be modeled by ab initio density functional theory (DFT) calculations. The results of nanoparticle characterization and catalytic testing can then be incorporated into the development of more accurate models for the theoretical prediction of nanoparticle structure and activity. This iterative process, summarized by the Conspectus graphic, leads to refinement of the theory and the prediction of better nanoparticle electrocatalyst candidates. This in turn leads to the next generation of more active electrocatalysts that can be used for a wide variety of applications.

STRUCTURE DETERMINATION

Dendrimer-Encapsulated Nanoparticles

DENs begin to provide a solution to some of the problems mentioned in the previous section. As shown in Figure 1a, DENs

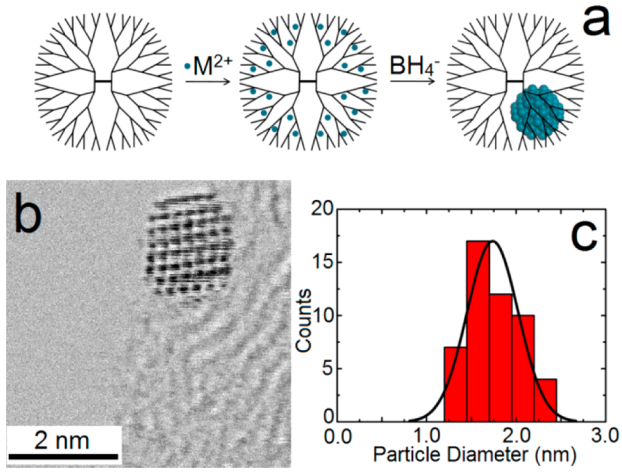

Figure 1. (a) General DENs synthesis scheme. (b) STEM image of a Au_{147} DEN and (c) size-distribution histogram of Au_{147} DENs. Adapted with permission from ref 58. Copyright 2013 The Royal Society of Chemistry.

are synthesized using a two-step templating method. First, metal ions are complexed to the interior of poly(amidoamine) (PAMAM) dendrimers. Second, a reducing agent is added which results in formation of a zerovalent metal nanoparticle that is sterically trapped within the dendrimer interior. This method leads to nanoparticles having an average size controlled by the metal-ion-to-dendrimer ratio present in the precursor solution. A representative aberration-corrected scanning transmission electron microscopy (ac-STEM) image of a Au_{147} DEN prepared within a sixth-generation, amine-terminated PAMAM dendrimer ($G6\text{-}NH_2$) is shown in Figure 1b, and a typical size-distribution histogram is presented in Figure 1c. In addition to its templating function, a second important aspect of the dendrimer is that it provides a scaffold for immobilization of DENs on surfaces, such as electrodes,[25] and also prevents direct contact between the surface and the encapsulated nanoparticles. The latter point is

DOI: 10.1021/acs.accounts.5b00125
Acc. Chem. Res. 2015, 48, 1351−1357

important when comparing experimental and theoretical findings, because support interactions introduce an additional level of complexity.

While the small size of DENs is an advantage for applying ab initio DFT calculations, it introduces the challenge of precisely characterizing nanoparticle structure. Common nanoparticle characterization techniques, such as X-ray diffraction (XRD), are more difficult to use and interpret than for nanoparticles just 1 nm larger. For example, XRD analysis requires a synchrotron source and pair distribution function (PDF) analysis.[26,27] Normal high-resolution transmission electron microscopy (TEM) is helpful, but ac-STEM yields far better resolution which is important for 1−2 nm particles.

More routine analytical methods also provide important information about DENs. For example, UV−vis spectroscopy is a good probe of specific interactions between metal ions and functional groups within the dendrimer (i.e., the DEN precursor), and it also provides some useful information about the DENs themselves. Electrochemistry also yields information about the identity of metals on the surface of DENs; for example, the presence of hydride waves can be correlated to Pt atoms.[28] More importantly, however, electrochemical measurements make it possible to directly measure electrocatalytic onset potentials and rates for comparison to theory.[29] While these routine techniques contribute to our understanding of DEN structure, an atomic-level understanding is best achieved using extended X-ray absorption fine structure (EXAFS) spectroscopy, which provides information about the local structure of nanoparticles.[30,31] EXAFS is, however, an averaging technique, so a high degree of monodispersity in size and composition is a prerequisite for deriving meaningful conclusions.[32] DENs meet these criteria, but as for XRD-PDF, synchrotron radiation and data fitting are necessary for obtaining EXAFS results.

DEN Shape Determination

Determining the overall shape of 1−2 nm particles using only experimental methods is difficult, but by including first-principles calculations in the analysis it is possible to draw definitive conclusions. For example, in one study from our groups,[33] three different polyhedral models for DEN shape were considered: cuboctahedron, truncated octahedron, and icosahedron. A simultaneous optimization was carried out for 147-atom Pt DENs by considering the goodness of fit to experimental PDFs as well as the nanoparticle energy from DFT. The goal of this type of optimization is to determine the nanoparticle structure that balances the minimization of the DFT energy while reducing the error between the experimental and theoretical PDFs. By introducing energy into the optimization problem, physically unreasonable structures that otherwise reproduce the experimental PDF can be discarded. Pareto optimal surfaces were generated that considered different weightings of the importance of reproducing the experimental PDF versus the theoretical DFT energy. The PDF analysis shows that face-centered cubic (FCC) structures (cuboctahedron and truncated octahedron) better reproduce the experimental results than an icosahedral structure, which is not FCC packed. When considering the energy of the structures calculated from DFT, the truncated octahedron shape was approximately 0.06 eV/atom lower in energy than the cuboctahedron, meaning it is the most likely shape. The important point is that this conclusion could not have been reached without a combined experimental/theoretical approach where the DFT energy was used to differentiate the cuboctahedron and truncated octahedron shapes.

Core@Shell DENs

Core@shell nanoparticles have received much recent attention due to their tunable properties and efficient utilization of the surface metal for catalysis.[34] Because of their structural uniformity and accessible surfaces, DENs are a useful construct for combining theory and experiment to better understand this important family of relatively complex materials. Accordingly, we discuss core@shell DENs next.

One method for preparing core@shell DENs involves the following two steps: (1) formation of the core using the approach shown in Figure 1a; and (2) immobilization of the core DENs onto an electrode surface followed by underpotential deposition (UPD) of a single atomic layer of a second metal. UPD is a process by which the depositing metal has a more favorable interaction with the substrate metal than it does with itself, leading to a lower electrodeposition potential for the first monolayer than for subsequent layers.[3] Importantly, the fact that UPD proceeds on electrode-immobilized DENs is a clear indication that the nanoparticle surface is easily accessible to solution species and that electron transfer between DENs and the electrode is unhindered.[35,36] Once the UPD layer is deposited, the core@shell nanoparticle is ready for characterization and electrocatalytic measurements. However, some shell metals cannot be deposited directly because they do not undergo UPD onto the core metal. In this case, it is necessary to displace a sacrificial shell metal with a more noble metal by galvanic exchange.[37] Importantly, galvanic exchange is a self-limiting process, so it is generally assumed that after galvanic replacement the geometry of the new shell is similar to the original UPD shell.[38,39]

To demonstrate the robustness of our combined experimental and theoretical treatment of the structure of core@shell DENs, we examined Pb UPD onto Au_{147} DENs.[39] Figure 2a shows cyclic voltammograms (CVs) for UPD of Pb^{2+} onto Au DENs. Pb is deposited onto the surface of the Au_{147} DEN cores as the potential is swept in the negative direction, and then it is removed when the potential is reversed. Following these experiments, the experimentally determined potentials of the peaks for the UPD of Pb were compared to potentials calculated by DFT. The red bars in Figure 2a represent the calculated potentials of Pb deposition on the Au cores while the blue bars show the calculated potentials of Pb monolayer oxidation. To establish an appropriate potential scale for the DFT results, the calculated energy for bulk deposition of Pb was assumed to be the same as the experimentally determined potential for multilayer deposition of bulk Pb onto the DEN core. The calculations revealed that Pb deposits on the Au (100) facets of the particles first, and then onto the (111) facets. Using currently available analytical tools, it would be impossible to draw this conclusion without these complementary calculations.

Structural Rearrangement of Core@Shell DENs

In addition to the heterogeneous electrochemical method discussed in the previous section, it is also possible to prepare core@shell DENs by a homogeneous chemical route. As we have learned, however, there are sometimes surprising and unexpected outcomes using this approach. In one case, we attempted to prepare Pd_{147}@Pt_{162} DENs using the following steps (Figure 3): (1) prepare a Pd_{147} core using the usual method; (2) add a hydride layer on the surface by bubbling H_2 gas into an aqueous solution of the Pd_{147} DENs; (3) use galvanic exchange to replace the hydride layer with Cu; (4) use galvanic exchange a second time to convert the Cu shell layer to Pt. Interestingly, this

DOI: 10.1021/acs.accounts.5b00125
Acc. Chem. Res. 2015, 48, 1351−1357

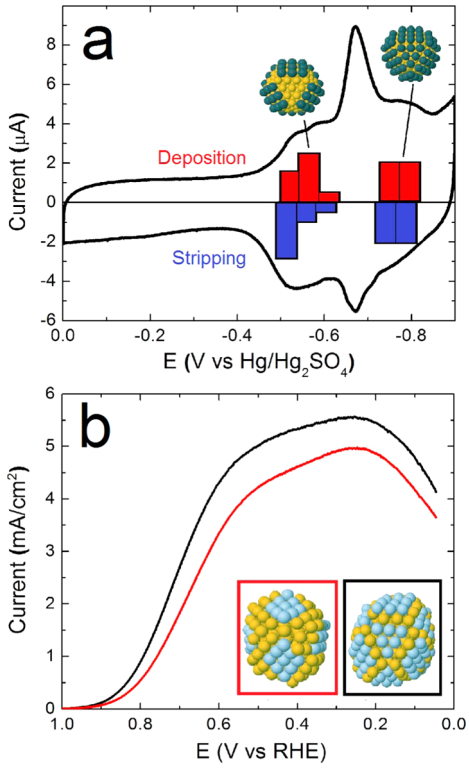

Figure 2. (a) CV showing the Pb UPD process at a Au_{147} DEN-modified glassy carbon electrode. DFT-calculated potentials for Pb deposition (red bars) and stripping (blue bars) are also shown. (b) ORR polarization curves for the indicated DEN-modified glassy carbon electrodes. Adapted with permission from ref 39. Copyright 2012 The Royal Society of Chemistry.

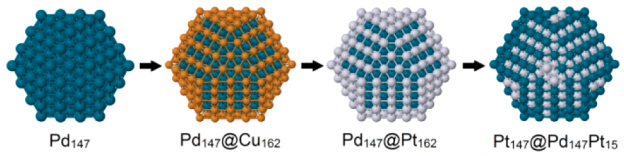

Figure 3. Synthetic scheme of formation of $Pd_{147}@Cu_{162}$, and the subsequent inversion after galvanic exchange of Pt for Cu. Reprinted with permission from ref 40. Copyright 2013 American Chemical Society.

procedure led to an inverted structure having a Pd shell rather than the desired Pd@Pt structure.[40]

DFT calculations carried out after the experimental analysis was complete indicated that the inverted $Pt_{147}@Pd_{147}Pt_{15}$ nanoparticle is the most thermodynamically stable structure. More importantly, DFT calculations provided insight into possible mechanisms for the rearrangement. Specifically, the segregation energy of the corner sites is the most negative, implying that Pt atoms in these corner sites have the greatest tendency to swap with neighboring Pd core atoms. This driving force at the corners of the particle may help to initiate the observed structural rearrangement. Another key finding was that inversion is an emergent property of these very small DENs, whereas larger (>3.5 nm) Pd@Pt nanoparticles are stable.[41,42]

■ ACTIVITY CORRELATIONS

Au@Pt DENs and the Electrocatalytic Oxygen Reduction Reaction (ORR)

The galvanic exchange of less noble UPD layers for Pt has been extensively studied by Adzic and co-workers for bulk surfaces[43] and for nanoparticles having diameters >4 nm.[34] In contrast to these earlier studies, core@shell DENs synthesized by the UPD method provide a well-defined and smaller experimental model that can be directly compared to DFT calculations and hence provide additional insights into their electrocatalytic properties.

For this study we prepared Au@Pt DENs via UPD of a shell (or partial shell) layer of Pb onto the Au core, followed by galvanic exchange of Pb for Pt (vide supra). We sought to understand how different amounts of Pt present on the Au core affects ORR activity.[39] To create the partial Pt shell DENs, Pb was initially electrodeposited onto only the Au(100) facets of Au_{147} cores by carefully controlling the electrode potential. DENs having complete shells were synthesized by electrodepositing Pb onto both the (100) and (111) facets prior to galvanic exchange.

We hypothesized that the partial Pt-shell catalysts would be less active for the ORR than DENs covered with a full shell, because the former would present only Pt(100) on their surface and Pt(100) is less active for the ORR than Pt(111).[44,45] Accordingly, we were surprised to find that both the partial and full Pt shell DENs exhibit nearly the same ORR activity as determined by the electrochemical measurements shown in Figure 2b. DFT-MD simulations were used to resolve this seeming inconsistency. As shown in Figure 2b (insets), these calculations revealed that the Pt(100) square facets rearrange into compressed (111) diamond orientations on both the full and partial shell structures.

Oxygen binding energy calculations were carried out for the reorganized Pt surfaces to assess their relative catalytic activities. The results showed that the diamond-shaped facets of the partial and full Pt shell systems have oxygen binding energies of −1.03 and −1.01 eV, respectively, while for the triangle-shaped facets of the full Pt shell catalyst it is only −0.7 eV. All of these values are higher than the binding energy of oxygen to bulk Pt (111), −1.55 eV, and therefore, they are less effective for breaking the dioxygen bond. Nevertheless, the nearly identical binding energies of oxygen on the diamond-shaped facets of the DENs, and their higher affinity for oxygen compared to the triangular facets, account for the similarity in activity of the partial and full Pt shell structures. Due to the small size of DENs, it would be impossible to use physical methods to characterize the structural changes that result in the diamond-shaped Pt features shown in Figure 2b. This is a perfect example, therefore, of how experiments and DFT-MD calculations can be coupled to interpret emergent experimental results.

Catalytic Oxidation of Formic Acid

The DFT-MD results discussed in the previous section revealed that Au@Pt DENs undergo a restructuring that renders them more catalytically active than we anticipated they would be a priori. This led us to hypothesize that it would be possible to use DFT-MD calculations to predict, *in advance of experiments*, how this restructuring (diamond-shaped facets) would affect a different reaction. We selected the oxidation of formic acid for this purpose. Electro-oxidation of formic acid to CO_2 on Pt electrocatalysts occurs via two mechanisms simultaneously: (1) through formation of a reactive intermediate (direct oxidation pathway), and (2) through formation of adsorbed CO (CO_{ads}) and subsequent oxidation of CO_{ads} to CO_2 (indirect oxidation pathway).[46] The indirect pathway is problematic, because it leads to poisoning of the Pt surface by CO_{ads}.

DFT-MD calculations showed that the structural deformation (diamond-shaped facets) of $Au_{147}@Pt$ DENs should lead to both

DOI: 10.1021/acs.accounts.5b00125
Acc. Chem. Res. 2015, 48, 1351−1357

slower dehydration of HCOOH and weaker binding of CO_{ads}. Both of these effects should improve the catalytic properties of the catalyst compared to Pt-only DENs. Note that this type of restructuring does not occur on larger particles. Previous reports of larger Au@Pt nanoparticle systems attribute the enhancement in formic acid oxidation to the suppression of CO_{ads}[47] and electronic interactions between the core and shell metal.[48,49]

Figure 4 shows CVs for formic acid (HCOOH) oxidation using Au_{147}, Pt_{147}, and Au_{147}@Pt DEN-modified glassy carbon

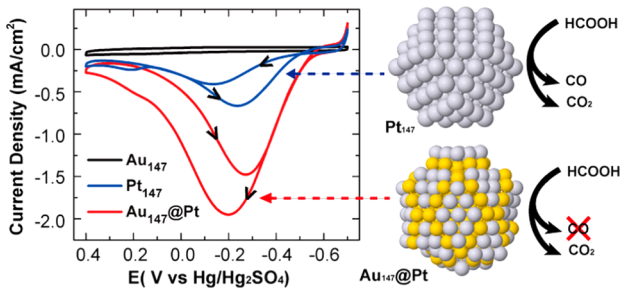

Figure 4. CVs for formic acid oxidation of Au_{147}, Pt_{147}, and Au_{147}@Pt DEN-modified glassy carbon electrodes along with optimized structures for the Pt-only DEN model (Pt_{147}) and the deformed partial-shell model ($Au@Pt_{dps}$), which is equivalent to Au_{147}@Pt_{102}. Reprinted with permission from ref 50. Copyright 2013 American Chemical Society.

electrodes in a 0.10 M $HClO_4$ electrolyte containing 0.10 M HCOOH. The Au_{147}@Pt DENs were made following the procedure described in the previous section, and therefore, we anticipated the same sort of restructuring that led to the diamond-shaped facets. As shown in Figure 4, the onset of HCOOH oxidation occurs at a lower potential on the Au_{147}@Pt DEN catalysts compared to the Au_{147} and Pt_{147} DENs. Additionally, the maximum current density for direct formic acid oxidation (at ~ −0.21 V) is significantly higher for the Au_{147}@Pt DENs. Most importantly, however, the CO_{ads} oxidation peak (~0.2 V) is nearly absent on the Au_{147}@Pt as compared to Pt_{147}, indicating that HCOOH is almost exclusively oxidized via the direct pathway. These experimental results are in full accord with the DFT calculations alluded to earlier: slower dehydration of HCOOH and weaker binding of CO_{ads}. It is these two factors, then, that account for the enhancement of the direct oxidation pathway and the lower CO poisoning observed in Figure 4.[50]

This study represents a good example (in fact, one of the few examples) of first-principles calculations making a prediction about an electrochemical process on a <2 nm catalyst that was subsequently proven by experiment to be correct. Moreover, the theoretical results also provide insights into the reaction pathway. The other important point is that direct experimental verification of the subtle structural changes in the DENs would be impossible. However, by confirming theoretical predictions about the reaction pathway (e.g., binding energies of reactants and intermediates) *engendered* by the restructuring of the DENs, confidence is gained in the unverifiable structural changes. This is an important conclusion and emphasizes the utility of using well-defined model systems that are fully compatible with first-principles calculations.

Alloy-Core@Shell DENs

Thus far we have shown that experimental electrocatalytic results can be rationalized with first-principles theory, and that the inverse is also true: theory can accurately lead experiments. Now we take this a step further and demonstrate that using even more complex catalysts, theory can still lead experiments down the right path. Specifically, we show here that the relative ORR activity of alloy-core@shell DENs of the form Pd_xAu_{140-x}@Pt is nearly perfectly predicted by DFT.

The roots of this work are found in our earlier reports of core@shell and random alloy nanoparticles.[51−54] We were also inspired by the work of others who demonstrated that alloy cores can be used to tune,[55] and in some cases stabilize,[56,57] the catalytic properties of the shell metal. To begin our study, we constructed theoretical models consisting of different core metal ratios (Pd:Au), and then calculated the binding energy of oxygen to the Pt shell.[29] We found that the strength of oxygen binding to the Pt-shell could be tuned, because Pd weakens oxygen binding while Au strengthens it. Accordingly, by controlling the ratio of the two core metals the oxygen binding to the Pt-shell could be optimized. Indeed, DFT calculations predicted that the peak activity for the ORR would be achieved at a core ratio of Au:Pd = 0.28:0.72 = 0.39. As shown in Figure 5, the optimal measured

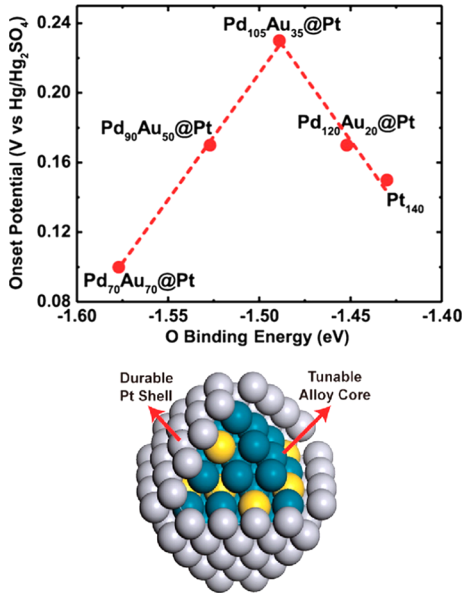

Figure 5. Onset potential for the ORR at Pd_xAu_{1-x}@Pt DENs measured by RDVs and plotted as a function of the corresponding oxygen binding energy calculated by DFT. The dashed line corresponds to the linear fit of the two branches of the activity volcano. Adapted with permission from ref 29. Copyright 2013 American Chemical Society.

activity was observed for $Pd_{105}Au_{35}$@Pt DENs (Au:Pd = 0.33). The close agreement between theory and experiment provides additional validation of the predictive ability of DFT calculations.

FUTURE DIRECTIONS

We plan to continue using theoretical methods to predict how catalyst structure will affect activity. A few specific questions we hope to address include the following. We now know that the use of binding energies as surrogate descriptors of activity is a viable approach for DENs. Are there other types of descriptors that can be used for this purpose? Is it possible to use multiple descriptors to tune reactivity? What is the scope of the alloy-core approach to tuning reactivity and particle stability? Can we remove the dendrimer from the DENs, and thereby invoke and predict catalytic behavior when the metal catalyst is in direct contract with the electrode surface? To what extent can we use first-principles theory to refine the interpretation of X-ray absorption

DOI: 10.1021/acs.accounts.5b00125
Acc. Chem. Res. 2015, 48, 1351−1357

spectra?[58] How general is the approach of confirming nanoparticle structural changes, which are too small to be directly observed using analytical methods, by comparing experimentally measured catalytic activities with those predicted by theory? Can ligands present on the nanoparticle surface be used to guide the structure and electronic properties of DENs to enhance their catalytic properties? Answers to all, or at least some, of these questions will be reported in due course.

AUTHOR INFORMATION

Corresponding Authors

*E-mail: henkelman@cm.utexas.edu. Telephone: 512-471-4179.
*E-mail: crooks@cm.utexas.edu. Telephone: 512-475-8674.

Notes

The authors declare no competing financial interest.

Biographies

Rachel M. Anderson received her B.S. in chemistry from Tufts University in 2010. She is currently a Ph.D. candidate at The University of Texas at Austin (UT-Austin) working on nanomaterials for catalysis applications.

David F. Yancey earned his B.S. in chemistry from the University of Michigan in 2009 and his Ph.D. from UT-Austin in 2013. His research focused on the synthesis and characterization of Au DENs. He is currently employed by The Dow Chemical Company in Midland, MI.

Liang Zhang received his B.S. in chemical physics from the University of Science and Technology of China and his Ph.D. in 2014 from UT-Austin under the supervision of Prof. Graeme Henkelman. His research interests are centered on the ab initio simulation of catalytic processes.

Samuel T. Chill received his Ph.D. in chemistry in 2014 from UT-Austin under the supervision of Graeme Henkelman. His research focused on the structural characterization of nanoparticles and the development of algorithms for long time-scale atomic simulations. He is currently employed by QuantumWise (Copenhagen, Denmark).

Graeme Henkelman received his Ph.D. from the University of Washington in 2001. He was a postdoctoral fellow at Los Alamos National Laboratory from 2002 to 2004 and is now a professor of chemistry at UT-Austin. His research interests include DFT and Monte Carlo studies of catalytic and energy storage materials.

Richard M. Crooks received his Ph.D. from UT-Austin and was a postdoctoral fellow at MIT in the 1980s. His independent career has been split between Texas A&M University and UT-Austin, where he is currently the Robert A. Welch Chair in Materials Chemistry. His research interests are in the fields of catalysis and analytical chemistry.

ACKNOWLEDGMENTS

We gratefully acknowledge support from the Chemical Sciences, Geosciences, and Biosciences Division, Office of Basic Energy Sciences, Office of Science, U.S. Department of Energy (Contract: DE-FG02-13ER16428). R.M.C. and G.H. thank the Robert A. Welch Foundation (Grants F-0032 and F-1841, respectively) for sustained support.

REFERENCES

(1) Goodman, D. W. Model Catalytic Studies over Metal Single Crystals. *Acc. Chem. Res.* **1984**, *17*, 194−200.
(2) Chang, S. C.; Weaver, M. J. In Situ Infrared Spectroscopy at Single-Crystal Metal Electrodes: An Emerging Link Between Electrochemical and Ultrahigh-Vacuum Surface Science. *J. Phys. Chem.* **1991**, *95*, 5391−5400.
(3) Herrero, E.; Buller, L. J.; Abruña, H. D. Underpotential Deposition at Single Crystal Surfaces of Au, Pt, Ag and Other Materials. *Chem. Rev.* **2001**, *101*, 1897−1930.
(4) Sachtler, J. W. A.; Somorjai, G. A. Influence of Ensemble Size on CO Chemisorption and Catalytic n-hexane Conversion by Au-Pt(111) Bimetallic Single-Crystal Surfaces. *J. Catal.* **1983**, *81*, 77−94.
(5) Zhou, W.-P.; Yang, X.; Vukmirovic, M. B.; Koel, B. E.; Jiao, J.; Peng, G.; Mavrikakis, M.; Adzic, R. R. Improving Electrocatalysts for O_2 Reduction by Fine-Tuning the Pt−Support Interaction: Pt Monolayer on the Surfaces of a $Pd_3Fe(111)$ Single-Crystal Alloy. *J. Am. Chem. Soc.* **2009**, *131*, 12755−12762.
(6) Taylor, C.; Kelly, R. G.; Neurock, M. Theoretical Analysis of the Nature of Hydrogen at the Electrochemical Interface Between Water and a Ni (111) Single-Crystal Electrode. *J. Electrochem. Soc.* **2007**, *154*, F55−F64.
(7) Nørskov, J. K.; Bligaard, T.; Rossmeisl, J.; Christensen, C. H. Towards the Computational Design of Solid Catalysts. *Nat. Chem.* **2009**, *1*, 37−46.
(8) Hernández, J.; Solla-Gullón, J.; Herrero, E.; Feliu, J. M.; Aldaz, A. In Situ Surface Characterization and Oxygen Reduction Reaction on Shape-Controlled Gold Nanoparticles. *J. Nanosci. Nanotechnol.* **2009**, *9*, 2256−2273.
(9) Nørskov, J. K.; Abild-Pedersen, F.; Studt, F.; Bligaard, T. Density Functional Theory in Surface Chemistry and Catalysis. *Proc. Natl. Acad. Sci. U. S. A.* **2011**, *108*, 937−943.
(10) Nørskov, J. K.; Rossmeisl, J.; Logadottir, A.; Lindqvist, L.; Kitchin, J. R.; Bligaard, T.; Jónsson, H. Origin of the Overpotential for Oxygen Reduction at a Fuel-Cell Cathode. *J. Phys. Chem. B* **2004**, *108*, 17886−17892.
(11) Rossmeisl, J.; Logadottir, A.; Nørskov, J. K. Electrolysis of Water on (Oxidized) Metal Surfaces. *Chem. Phys.* **2005**, *319*, 178−184.
(12) Man, I. C.; Su, H.-Y.; Calle-Vallejo, F.; Hansen, H. A.; Martínez, J. I.; Inoglu, N. G.; Kitchin, J.; Jaramillo, T. F.; Nørskov, J. K.; Rossmeisl, J. Universality in Oxygen Evolution Electrocatalysis on Oxide Surfaces. *ChemCatChem* **2011**, *3*, 1159−1165.
(13) Ferrin, P.; Nilekar, A. U.; Greeley, J.; Mavrikakis, M.; Rossmeisl, J. Reactivity Descriptors for Direct Methanol Fuel Cell Anode Catalysts. *Surf. Sci.* **2008**, *602*, 3424−3431.
(14) Esposito, D. V.; Hunt, S. T.; Kimmel, Y. C.; Chen, J. G. A New Class of Electrocatalysts for Hydrogen Production from Water Electrolysis: Metal Monolayers Supported on Low-Cost Transition Metal Carbides. *J. Am. Chem. Soc.* **2012**, *134*, 3025−3033.
(15) Johnson, G. E.; Wang, C.; Priest, T.; Laskin, J. Monodisperse Au_{11} Clusters Prepared by Soft Landing of Mass Selected Ions. *Anal. Chem.* **2011**, *83*, 8069−8072.
(16) Oja, S. M.; Wood, M.; Zhang, B. Nanoscale Electrochemistry. *Anal. Chem.* **2013**, *85*, 473−486.
(17) Sambur, J. B.; Chen, P. Approaches to Single-Nanoparticle Catalysis. *Annu. Rev. Phys. Chem.* **2014**, *65*, 395−422.
(18) Crooks, R. M.; Zhao, M.; Sun, L.; Chechik, V.; Yeung, L. K. Dendrimer-Encapsulated Metal Nanoparticles: Synthesis, Characterization, and Applications to Catalysis. *Acc. Chem. Res.* **2001**, *34*, 181−190.
(19) Niu, Y.; Crooks, R. M. Dendrimer-Encapsulated Metal Nanoparticles and Their Applications to Catalysis. *C. R. Chim.* **2003**, *6*, 1049−1059.
(20) Scott, R. W. J.; Wilson, O. M.; Crooks, R. M. Synthesis, Characterization, and Applications of Dendrimer-Encapsulated Nanoparticles. *J. Phys. Chem. B* **2005**, *109*, 692−704.
(21) Bronstein, L. M.; Shifrina, Z. B. Dendrimers As Encapsulating, Stabilizing, or Directing Agents for Inorganic Nanoparticles. *Chem. Rev.* **2011**, *111*, 5301−5344.
(22) Myers, V. S.; Weir, M. G.; Carino, E. V.; Yancey, D. F.; Pande, S.; Crooks, R. M. Dendrimer-Encapsulated Nanoparticles: New Synthetic and Characterization Methods and Catalytic Applications. *Chem. Sci.* **2011**, *2*, 1632−1646.
(23) Zheng, J.; Petty, J. T.; Dickson, R. M. High Quantum Yield Blue Emission from Water-Soluble Au_8 Nanodots. *J. Am. Chem. Soc.* **2003**, *125*, 7780−7781.

DOI: 10.1021/acs.accounts.5b00125
Acc. Chem. Res. 2015, 48, 1351−1357

(24) Bao, Y.; Zhong, C.; Vu, D. M.; Temirov, J. P.; Dyer, R. B.; Martinez, J. S. Nanoparticle-Free Synthesis of Fluorescent Gold Nanoclusters at Physiological Temperature. *J. Phys. Chem. C* **2007**, *111*, 12194−12198.
(25) Ye, H.; Crooks, R. M. Electrocatalytic O_2 Reduction at Glassy Carbon Electrodes Modified with Dendrimer-Encapsulated Pt Nanoparticles. *J. Am. Chem. Soc.* **2005**, *127*, 4930−4934.
(26) Petkov, V.; Bedford, N.; Knecht, M. R.; Weir, M. G.; Crooks, R. M.; Tang, W.; Henkelman, G.; Frenkel, A. Periodicity and Atomic Ordering in Nanosized Particles of Crystals. *J. Phys. Chem. C* **2008**, *112*, 8907−8911.
(27) Knecht, M. R.; Weir, M. G.; Myers, V. S.; Pyrz, W. D.; Ye, H.; Petkov, V.; Buttrey, D. J.; Frenkel, A. I.; Crooks, R. M. Synthesis and Characterization of Pt Dendrimer-Encapsulated Nanoparticles: Effect of the Template on Nanoparticle Formation. *Chem. Mater.* **2008**, *20*, 5218−5228.
(28) Yancey, D. F.; Carino, E. V.; Crooks, R. M. Electrochemical Synthesis and Electrocatalytic Properties of Au@Pt Dendrimer-Encapsulated Nanoparticles. *J. Am. Chem. Soc.* **2010**, *132*, 10988−10989.
(29) Zhang, L.; Iyyamperumal, R.; Yancey, D. F.; Crooks, R. M.; Henkelman, G. Design of Pt-Shell Nanoparticles with Alloy Cores for the Oxygen Reduction Reaction. *ACS Nano* **2013**, *7*, 9168−9172.
(30) Frenkel, A. Solving the 3D Structure of Metal Nanoparticles. *Z. Kristallogr.* **2007**, *222*, 605−611.
(31) Frenkel, A. I. Applications of Extended X-Ray Absorption Fine-Structure Spectroscopy to Studies of Bimetallic Nanoparticle Catalysts. *Chem. Soc. Rev.* **2012**, *41*, 8163−8178.
(32) Frenkel, A. I.; Yevick, A.; Cooper, C.; Vasic, R. Modeling the Structure and Composition of Nanoparticles by Extended X-Ray Absorption Fine-Structure Spectroscopy. *Annu. Rev. Anal. Chem.* **2011**, *4*, 23−39.
(33) Welborn, M.; Tang, W.; Ryu, J.; Petkov, V.; Henkelman, G. A Combined Density Functional and X-Ray Diffraction Study of Pt Nanoparticle Structure. *J. Chem. Phys.* **2011**, *135*, 014503.
(34) Wang, J. X.; Inada, H.; Wu, L.; Zhu, Y.; Choi, Y.; Liu, P.; Zhou, W.-P.; Adzic, R. R. Oxygen Reduction on Well-Defined Core−Shell Nanocatalysts: Particle Size, Facet, and Pt Shell Thickness Effects. *J. Am. Chem. Soc.* **2009**, *131*, 17298−17302.
(35) Chazalviel, J.-N.; Allongue, P. On the Origin of the Efficient Nanoparticle Mediated Electron Transfer across a Self-Assembled Monolayer. *J. Am. Chem. Soc.* **2011**, *133*, 762−764.
(36) Barfidokht, A.; Ciampi, S.; Luais, E.; Darwish, N.; Gooding, J. J. Distance-Dependent Electron Transfer at Passivated Electrodes Decorated by Gold Nanoparticles. *Anal. Chem.* **2013**, *85*, 1073−1080.
(37) Brankovic, S. R.; Wang, J. X.; Adzic, R. R. Metal Monolayer Deposition by Replacement of Metal Adlayers on Electrode Surfaces. *Surf. Sci.* **2001**, *474*, L173−L179.
(38) Carino, E. V.; Kim, H. Y.; Henkelman, G.; Crooks, R. M. Site-Selective Cu Deposition on Pt Dendrimer-Encapsulated Nanoparticles: Correlation of Theory and Experiment. *J. Am. Chem. Soc.* **2012**, *134*, 4153−4162.
(39) Yancey, D. F.; Zhang, L.; Crooks, R. M.; Henkelman, G. Au@Pt Dendrimer Encapsulated Nanoparticles As Model Electrocatalysts for Comparison of Experiment and Theory. *Chem. Sci.* **2012**, *3*, 1033−1040.
(40) Anderson, R. M.; Zhang, L.; Loussaert, J. A.; Frenkel, A. I.; Henkelman, G.; Crooks, R. M. An Experimental and Theoretical Investigation of the Inversion of Pd@Pt Core@Shell Dendrimer-Encapsulated Nanoparticles. *ACS Nano* **2013**, *7*, 9345−9353.
(41) Taufany, F.; Pan, C.-J.; Rick, J.; Chou, H.-L.; Tsai, M.-C.; Hwang, B.-J.; Liu, D.-G.; Lee, J.-F.; Tang, M.-T.; Lee, Y.-C.; Chen, C.-I. Kinetically Controlled Autocatalytic Chemical Process for Bulk Production of Bimetallic Core−Shell Structured Nanoparticles. *ACS Nano* **2011**, *5*, 9370−9381.
(42) Frenkel, A. I.; Wang, Q.; Sanchez, S. I.; Small, M. W.; Nuzzo, R. G. Short Range Order in Bimetallic Nanoalloys: An Extended X-ray Absorption Fine Structure Study. *J. Chem. Phys.* **2013**, *138*, 064202.
(43) Lima, F. H. B.; Zhang, J.; Shao, M. H.; Sasaki, K.; Vukmirovic, M. B.; Ticianelli, E. A.; Adzic, R. R. Catalytic Activity−d-Band Center Correlation for the O_2 Reduction Reaction on Platinum in Alkaline Solutions. *J. Phys. Chem. C* **2007**, *111*, 404−410.
(44) Viswanathan, V.; Hansen, H. A.; Rossmeisl, J.; Nørskov, J. K. Universality in Oxygen Reduction Electrocatalysis on Metal Surfaces. *ACS Catal.* **2012**, *2*, 1654−1660.
(45) Kondo, S.; Nakamura, M.; Maki, N.; Hoshi, N. Active Sites for the Oxygen Reduction Reaction on the Low and High Index Planes of Palladium. *J. Phys. Chem. C* **2009**, *113*, 12625−12628.
(46) Capon, A.; Parson, R. The Oxidation of Formic Acid at Noble Metal Electrodes: I. Review of Previous Work. *J. Electroanal. Chem. Interfacial Electrochem.* **1973**, *44*, 1−7.
(47) Kristian, N.; Yan, Y.; Wang, X. Highly Efficient Submonolayer Pt-Decorated Au Nano-Catalysts for Formic Acid Oxidation. *Chem. Commun.* **2008**, 353−355.
(48) Park, I.-S.; Lee, K.-S.; Choi, J.-H.; Park, H.-Y.; Sung, Y.-E. Surface Structure of Pt-Modified Au Nanoparticles and Electrocatalytic Activity in Formic Acid Electro-Oxidation. *J. Phys. Chem. C* **2007**, *111*, 19126−19133.
(49) Zhang, G.-R.; Zhao, D.; Feng, Y.-Y.; Zhang, B.; Su, D. S.; Liu, G.; Xu, B.-Q. Catalytic Pt-on-Au Nanostructures: Why Pt Becomes More Active on Smaller Au Particles. *ACS Nano* **2012**, *6*, 2226−2236.
(50) Iyyamperumal, R.; Zhang, L.; Henkelman, G.; Crooks, R. M. Efficient Electrocatalytic Oxidation of Formic Acid Using Au@Pt Dendrimer-Encapsulated Nanoparticles. *J. Am. Chem. Soc.* **2013**, *135*, 5521−5524.
(51) Lu, C.-Y.; Henkelman, G. Role of Geometric Relaxation in Oxygen Binding to Metal Nanoparticles. *J. Phys. Chem. Lett.* **2011**, *2*, 1237−1240.
(52) Tang, W.; Henkelman, G. Charge Redistribution in Core-Shell Nanoparticles to Promote Oxygen Reduction. *J. Chem. Phys.* **2009**, *130*, 194504.
(53) Tang, W.; Zhang, L.; Henkelman, G. Catalytic Activity of Pd/Cu Random Alloy Nanoparticles for Oxygen Reduction. *J. Phys. Chem. Lett.* **2011**, *2*, 1328−1331.
(54) Zhang, L.; Henkelman, G. Tuning the Oxygen Reduction Activity of Pd Shell Nanoparticles with Random Alloy Cores. *J. Phys. Chem. C* **2012**, *116*, 20860−20865.
(55) Koenigsmann, C.; Sutter, E.; Adzic, R. R.; Wong, S. S. Size- and Composition-Dependent Enhancement of Electrocatalytic Oxygen Reduction Performance in Ultrathin Palladium−Gold ($Pd_{1-x}Au_x$) Nanowires. *J. Phys. Chem. C* **2012**, *116*, 15297−15306.
(56) Sasaki, K.; Naohara, H.; Choi, Y.; Cai, Y.; Chen, W.-F.; Liu, P.; Adzic, R. R. Highly Stable Pt Monolayer on PdAu Nanoparticle Electrocatalysts for the Oxygen Reduction Reaction. *Nat. Commun.* **2012**, *3*, 1115.
(57) Koenigsmann, C.; Sutter, E.; Chiesa, T. A.; Adzic, R. R.; Wong, S. S. Highly Enhanced Electrocatalytic Oxygen Reduction Performance Observed in Bimetallic Palladium-Based Nanowires Prepared under Ambient, Surfactantless Conditions. *Nano Lett.* **2012**, *12*, 2013−2020.
(58) Yancey, D. F.; Chill, S. T.; Zhang, L.; Frenkel, A. I.; Henkelman, G.; Crooks, R. M. A Theoretical and Experimental Examination of Systematic Ligand-Induced Disorder in Au Dendrimer-Encapsulated Nanoparticles. *Chem. Sci.* **2013**, *4*, 2912−2921.

DOI: 10.1021/acs.accounts.5b00125
Acc. Chem. Res. 2015, 48, 1351−1357